Investigation of the Swelling Response and Drug Loading of Ionic Microgels: The Dependence on Functional Group Composition

Gary M. Eichenbaum,[†] Patrick F. Kiser,[†,‡] Dipak Shah,[†] Sidney A. Simon,[§] and David Needham*[,†]

Department of Mechanical Engineering and Materials Science, Duke University, Durham, North Carolina 27708; Access Pharmaceuticals, Dallas, Texas 75207; and Department of Neurobiology, Duke University Medical Center, Durham, North Carolina 27710

Received May 28, 1999; Revised Manuscript Received October 11, 1999

ABSTRACT: Spherical micron-sized (4−7 μm diameter) poly(methacrylic acid-*co*-nitrophenyl acrylate) microgels were synthesized by precipitation polymerization and selectively derivatized with carboxylic acid, glutamic acid, hydroxamic acid, sulfonic acid, and ethanol functional groups in five separate post-polymerization reactions. The pH and NaCl induced swelling response, drug loading, capacity ("capacity" = total number of functional ionic groups that bind protons), and density of the five different composition anionic microgels, each containing a different functional group as well as a baseline of carboxylic acid groups, were measured. Using the micropipet flow technique, it was found that the pH range of the swelling response for the five different microgel compositions shifted by an amount that was proportional to the solution pK_a's of their functional groups. The degree of drug loading increased in proportion to the microgels' capacity. However, the drug loading did not decrease proportionately when the capacity was lowered.

Introduction

Ionic hydrogels have been engineered to have specific pH and ion responsive material properties.[1−3] The polymer repeat unit composition and the type of pendant groups on the polymer backbone of an ionic hydrogel's polymer matrix play a crucial role in determining the pH range, the degree of swelling, the density, and the capacity ("capacity" = number of functional ionic groups as measured by proton uptake) of the microgels.[2,4] The material properties of ionic hydrogels are also dependent on the different properties and geometries of pendant groups.[2]

In this paper we have explored how changing the functional groups affects various properties of ionic microgels. The term "ionic microgel" refers to a spherical, micrometer in diameter, covalently cross-linked, high molecular weight polymer matrix that has fixed ionic groups bound to its backbone. From an experimental perspective, a motivation for working with ionic microgels was to take advantage of the fact that microgels in the micrometer size range show a very rapid response (i.e., 0.5 s to reach equilibrium) to changing environmental conditions.[5]

From a biomedical applications standpoint, the microgels' small size permits them to travel in the bloodstream and even be targeted to certain diseased tissues outside the bloodstream.[6] An understanding of the influence that fixed ionic groups have on a microgels' material and molecular exchange properties is crucial for making new microgels that will be used in specific drug delivery and therapeutic applications.

For the materials engineering of new ionic microgels we draw upon earlier work that has been done on organic ion-exchange resins and ionic slab gels.[2,3,7−12] Organic ion-exchange resins are similar to polymer hydrogels in that they have hydrophilic fixed ionic groups on their backbone, but unlike hydrogels they have a hydrophobic matrix. It is well established for macroscopic ion-exchange resins that their behavior is primarily determined by the chemical nature of their fixed ionic groups.[7] The number and type of fixed ionic groups on the resin matrix determine their capacity and selectivity, respectively.

In this paper, by measuring the effect of the functional group composition on swelling and drug loading, we built on our previous work in which we examined the effect of ionic microgel cross-linking density on swelling and drug/protein loading.[13] Our goals here were to show that (1) derivatizing microgels with functional groups that had higher or lower pK_a's would increase and decrease, respectively, the pH range of the microgels' swelling response; (2) increasing or decreasing the concentration of fixed ionic groups in the microgels would increase and decrease, respectively, their exchange capacity as well as the magnitude of their swelling response; and (3) incorporating functional groups in the microgels that were more or less selective for different ionic molecules would increase and decrease, respectively, the selectivity of the microgels for loading these molecules.

To achieve these goals, we synthesized micron-sized (4−7 μm diameter) poly(methacrylic acid-*co*-nitrophenyl acrylate) (PMAA) microgels by precipitation polymerization. To selectively modify the compositions of the PMAA microgels, we have developed a new set of post-polymerization reactions. One significant advantage to modifying the composition of the hydrogel matrix after the polymerization was quenched was that all modifications could be made to hydrogels that had the same starting structure. In each reaction a different functional group (carboxylic acid, glutamic acid, hydroxamic

[†] Duke University.
[‡] Access Pharmaceuticals.
[§] Duke University Medical Center.
* To whom correspondence should be addressed.

10.1021/ma9908393 CCC: $18.00
Published on Web 12/08/1999

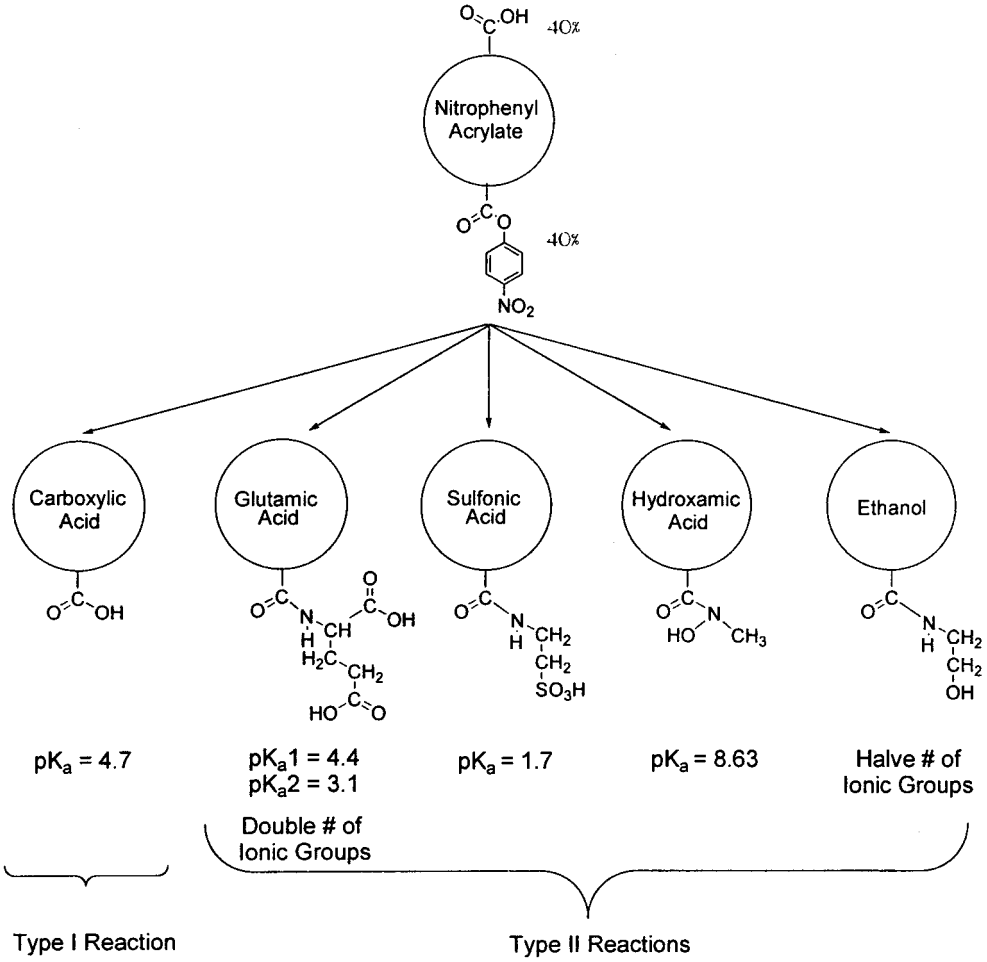

Figure 1. Schematic diagram of the five different microgel compositions that were made from the NPA microgels. On the basis of the feed ratio that was used in the polymerization of the NPA microgels (40% methacrylic acid polymer repeat units, 20% methylenebis(acrylamide) cross-linker, and 40% of the functional group shown), a maximum of 40% of the polymer repeat units on the microgel were available for modification. The carboxylic acid microgels were obtained by the type I and the other four compositions were obtained by the type II reactions described below. The pK_a's for each of the functional groups is shown.

acid, sulfonic acid, and ethanol) was covalently bound to the polymer backbone (in place of the nitrophenol that was connected to one of the starting polymer repeat units, Figure 1). These five functional groups were selected on the basis of differences in their solution pK_a's, number of ionic groups per polymer repeat unit, and/or ion selectivity. By characterizing the effects of these functional groups on the microgels' pH, ion, and drug loading properties, we could determine how to control the range and capacity of the microgels' response. Whenever possible, all compositions were characterized with regard to their apparent pK_a (by aqueous bulk titration), volume response as a function of pH and NaCl concentration, swollen density, and drug loading properties. For the drug loading studies we used two local anesthetics, benzylamine and dibucaine, and the anticancer drug doxorubicin. To explain the pH swelling response of the carboxylic acid, glutamic acid, and ethanol microgels, a model based on Flory−Huggins thermodynamic theory for network swelling was applied.

Materials and Methods

Poly(methacrylic acid-*co*-nitrophenyl acrylate) Microgel Synthesis. All of the microgels were synthesized by modifying the method developed by Kawaguchi.[14,15] The starting materials for the poly(methacrylic acid-*co*-nitrophenyl acrylate) microgels consisted of 4-nitrophenyl acrylate monomer (NPA) (2.07 g), methacrylic acid monomer (MAA) (0.861 g), methylenebis(acrylamide) cross-linker (MBAM) (0.771 g), azobis(isobutyronitrile) (AIBN) (1.5 g), and ethanol (EtOH) (40 g). The monomer feed ratio consisted of four methacrylic acid monomers for every one methylenebis(acrylamide) cross-linker.

MBAM (Aldrich) was recrystallized twice from methanol at 50 °C, and NPMA was recrystallized from methanol and cooled to −60 °C before collecting the crystals. AIBN (Aldrich) was recrystallized twice from chloroform. MAA (Aldrich) was twice distilled at 30 °C under vacuum. All monomers and initiators were stored under argon at −20 °C. The monomers and initiator were dissolved in EtOH. Because nitrophenol acts as a chain transfer agent, an equivalent molar mass of initiator to the amount of NPA monomer was required.[15] The reactions were degassed at room temperature for 20 min by bubbling argon into the alcohol solution. The flask containing argon was immersed in a mineral oil bath, and the reaction medium was warmed to 60 °C, whereupon solid AIBN was added to the reaction. Within 3 min after the addition of the initiator, the solution became a cloudy dispersion of particles. The reactions were left unstirred, as stirring was found to reduce the particle size. The reaction was run for 3 h. It was left standing until it reached room temperature. The sample was pelleted by centrifugation (2000 RCF) and then resuspended in fresh ethanol. This process was repeated five times, and then the sample was dried to a constant weight (100 °C, 0.1 Torr for 12 h).

Post-Polymerization Modifications. Here we describe the methods that were developed to make post-polymerization compositional modifications to the NPA microgels (synthesis described above). The goal of the post polymerization reactions was to replace the chemically reactive nitrophenol groups (40% of the monomers based upon the feed ratio), which were incorporated into the microgels during their synthesis, with one of five different functional groups: ethanol, carboxylic acid, methylhydroxamic acid, sulfonic acid, and glutamic acid (Figure 1). This resulted in the synthesis of five new and different microgel compositions. Because the monomer feed ratio that was used in the polymerizations was 2:2:1 (methacrylic acid monomers to nitrophenyl monomers to cross-linking monomers), a maximum of 40% of the polymer repeat units were available for compositional modification by nitrophenol replacement.

A different method was used to functionalize the microgels with carboxylic acid groups (type I reaction in Figure 1) than was used to functionalize the microgels with the ethanol, hydroxamic acid, sulfonic acid, and glutamic acid groups (type II reaction in Figure 1). The details of the two methods that were used are described below.

Type I Reaction: Carboxylic Acid Derivatization. To completely derivatize the microgels with carboxyl groups, the dried reaction product of NPA microgels (which had been washed with THF) was suspended for 5 h in 50 mL of 1 M NaOH. During this time a hydrolysis reaction occurred. In this reaction hydroxide anions attacked the carbonyl of the NPA polymer repeat units, and nitrophenol was released into solution.

To measure the amount of nitrophenol released in this reaction, a spectrophotometric calibration curve of nitrophenol absorbance at 400 nm versus nitrophenol concentration in pH 10.0 buffer (a pH at which the nitrophenol is deprotonated) was made. A molar extinction coefficient of 2.05×10^4 (M^{-1}) was obtained. By measuring the nitrophenol absorbance in the supernatant of the hydrolysis reaction, the extent of nitrophenol replacement by carboxylic acids during the reaction and the total moles of nitrophenol that were initially bound per mg of microgels were quantitatively determined.

This hydrolysis reaction produced a new copolymer composition of methacrylic acid, acrylic acid, and methylenebis(acrylamide). To remove the products of the hydrolysis, the resulting microgel suspension was centrifuged and washed in distilled water four times**.** This resulted in a relatively monodisperse (average diameter of 5 ± 1 μm (SD) in ethanol and measured as described below). Finally, the beads were stored at 4 °C in deionized water.

Type II Reaction: Ethanol, Methylhydroxamic Acid, Sulfonic Acid, and Glutamic Acid. The goal of this set of reactions was to replace the nitrophenol group on the NPA microgels with one of four different nucleophilic molecules: aminoethanol, *N*-methylhydroxylamine, glutamic acid diethyl ester, and taurine. Because each of these molecules contains a terminal amine, they can be derivatized to the microgels using a nucleophilic displacement reaction (assuming that it is not sterically hindered from reaching the nitrophenyl esters). The amount of nucleophile that was used in all of these reactions was set at 10 times the number of moles of nitrophenol groups per milligram of beads (as determined in a control type I reaction). It was necessary to run the reactions in anhydrous DMF to prevent the base-catalyzed hydrolysis reaction (type I, which was favorable under aqueous conditions) from preferentially occurring.

Triethylamine (a strong nonreactive base) was included in all four reactions for two reasons: (1) to deprotonate the amines on the four molecules and convert them into a nucleophilic form, which would attack the nitrophenyl ester on the microgel matrix, and (2) to bind to the nitrophenol once it was released so that it would not associate with the unreacted nucleophile and prevent it from reacting. The amount of triethylamine that was used in each reaction was set at 2 times the molar equivalents of nucleophile plus the total nitrophenol released (as was measured by the type I hydrolysis reaction). The number of molar equivalents of nucleophile that were used in each reaction was set at 10 times the total number of moles of nitrophenol per milligram of microgels (as again was measured from the type I hydrolysis reaction).

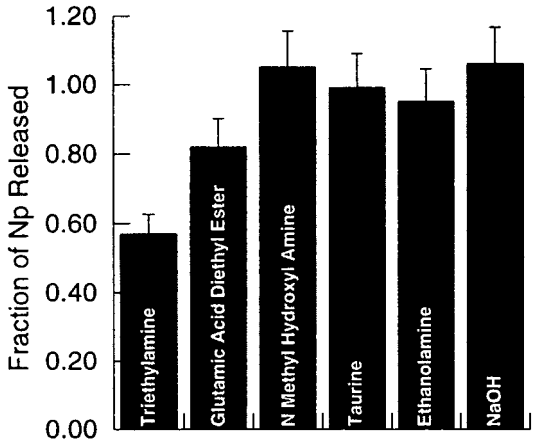

Figure 2. Plot showing the percentage of nitrophenol released from the microgels for each of the five different post-polymerization reactions.

Unlike the hydrolysis reaction, in the type II reactions it was not possible to quantitatively determine the extent of nucleophilic replacement of nitrophenol by measuring the amount of nitrophenol released into the bulk solution. This was because a side reaction was observed to occur, in which nitrophenol was released from the microgels in the presence of triethylamine alone (no nucleophile present). The amount of nitrophenol released was 57% of the total nitrophenol released in the case of the hydrolysis reaction by NaOH in water. Because triethylamine cannot react and replace the nitrophenyl ester directly, it was hypothesized that the triethylamine had catalyzed an intrapolymer reaction in which carboxylic acid groups from the methacrylic acid polymer repeat units reacted with neighboring nitrophenyl esters to form anhydride intermediates. There is strong evidence to support this hypothesis;[16,17] this reaction has been observed and its kinetics studied extensively for the case of linear copolymers of methacrylic acid and nitrophenyl acrylate and methacrylate.

From the perspective of the original goal, i.e., modifying the microgels with the four different functional groups, this side reaction was not a problem since the anhydride which forms, like the nitrophenyl ester, was also susceptible to attack by the four nucleophiles. To take into account the fact that the kinetics of the nucleophilic attack of the anhydride might be slower than the nucleophilic attack of the nitrophenyl ester, all four of these reactions were heated to 60 °C and run for 72 h. The amount of nitrophenol released in these reactions was measured spectrophotometrically. To remove the products of the hydrolysis, the resulting microgel suspension was centrifuged and washed three times with 50 mL of ethanol. To determine whether any additional nitrophenyl esters had remained unreacted after this reaction, the resulting microgels were pelleted and resuspended in 50 mL of 1 M NaOH for 2 h, and the amount of additional nitrophenol released was measured spectrophotometrically. Figure 2 shows a plot of the fraction of total nitrophenol released from the microgels during each of the five post-polymerization reactions. With the exception of the glutamic acid microgel reactions in which 0.82 was released, 1.00 of the nitrophenol was released in all of the other reactions. To determine whether all of the triethylamine was washed from the microgels after these reactions, hydrogen, carbon, and nitrogen combustion analysis was performed (Atlantic Microlabs, Norcross, GA). After four washes with ethanol, the amount of nitrogen in the microgels decreased to a steady-state value that was equal to the amount of nitrogen in a control sample, indicating that all of the triethylamine had been removed.

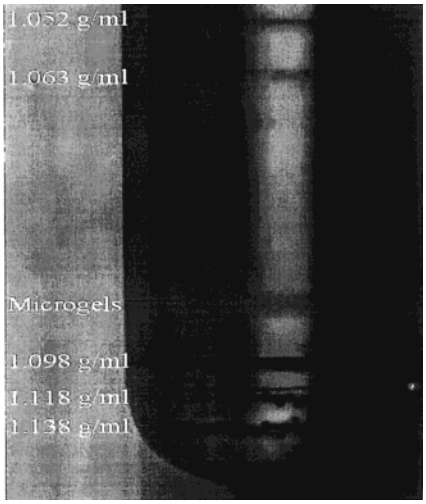

Figure 3. Video image of a centrifuge tube containing the carboxylic acid microgels and the density marker beads in a Percoll sucrose gradient.

Size Distribution. Images of 50 microgels from each of the five compositions suspended in different pH buffer solutions were recorded using a camera interfaced with an interference contrast microscope. From measurements of the diameter of the 50 microgels in these images the volume distribution was obtained. All bulk volume measurement data are presented as the mean volume ± SD.

Swollen Microgel Density Measurements at pH = 7.5. We used a Percoll density gradient that was calibrated with marker bead standards (Sigma Chemical Company, St. Louis, MO) to measure the density of the five different microgel compositions in their fully swollen state. This technique has been commonly used to obtain the density of cells,[18,19] and here we found it readily adaptable for density measurements of microgels. To obtain the appropriate density range for measurements of each of the five microgel compositions, Percoll was mixed in a 1:1 volume ratio with 0.25 M sucrose at a pH of 7.5. A sucrose-based density gradient was selected because, being a nonelectrolyte, sucrose did not change the volume of the microgels from their maximum volume at this concentration and pH.

Marker bead standards and microgels (0.5 mg) were added to 1 mL aliquots of the Percoll/sucrose solutions. The mixtures were vortexed and placed in polysaccharide centrifuge tubes (Beckman). The microgels and marker beads were then placed in the centrifugal field of an airfuge (Beckman) at 25 000 rpm for 25 min. Thin bands of different color marker beads and a single white band of the microgels were observed in each centrifuge tube. To measure the relative locations of the marker bead standards and the microgels, an image of the tube was recorded on videocassette (Figure 3). Video calipers (model 305, Vista Electronics, La Mesa, CA) were used to measure the distances between the known density standards and microgels from a fixed reference point on the video image. By plotting density versus distance of the marker bead standards and fitting a polynomial to the distance data, the unknown density of the microgels could be interpolated. The average standard deviation on the density measurements was ±0.001 g/cm^3.

Solutions Used in the Measurements of the Volume Response. Buffered sodium citrate and phosphate buffer solutions were used in the measurements of the equilibrium swelling response (Q) of individual microgels. For the combined pH and NaCl concentration experiments, the citrate buffer solutions contained 10 mM citrate and ranged from pH 2.5 to 6.6 in approximately 0.2 pH unit increments. The phosphate buffer solutions contained 10 mM phosphate and ranged from pH 6.2 to 7.8. There were no differences between the microgel volumes in 10 mM phosphate and 10 mM citrate buffer at the same pH. For measurements of Q of the microgels in response to changes in NaCl concentration, the solutions contained 0.1 mM phosphate buffers with 0.001, 0.01, 0.1, 1.0, and 5.0 M NaCl, all at pH 7.8.

Micromanipulation of Microgels. The micropipet flow technique has been described in detail elsewhere.[5] Briefly, this technique is a useful method for manipulating and observing the pH and ion induced swelling response of individual microgels that have a diameter greater than 1 μm. All micropipet manipulation based measurements were repeated on four different microgels of all five compositions. Note that by using this technique to measure the swelling response of single microgels, the errors associated with diameter measurements of a bulk sample of microgels, as a result of microgel polydispersity, were significantly reduced.[5]

Molecular and Drug Loading. To measure the bulk loading of cationic anesthetics and an anticancer drug into the different composition microgels, we chose three monovalent, cationic molecules that have increasing molecular weight and complexity. They were benzylamine hydrochloride (MW 143.6 g/mol), dibucaine hydrochloride (MW 379.9 g/mol), and doxorubicin hydrochloride (MW 580.0 g/mol) (obtained from Sigma Chemical Company, St. Louis, MO). The maximum wavelengths that were used for the absorbance measurements of benzylamine, dibucaine, and doxorubicin were 206.0, 208.0, and 481.5 nm, respectively.

Fifty microliters of each of the different composition microgels (prepared at 1 mg/mL in deionized water) was combined in separate vessels with 450 μL aliquots of 3 mM benzylamine in deionized water, 3 mM doxorubicin in 10 mM TRIS buffer, and 1.5 mM dibucaine in deionized water. The concentration of each cationic molecule was set at a sufficient level to achieve the maximum loading. The maximum loading level was determined by removing the supernatant, resuspending the microgels in fresh stock solution, and then measuring for additional uptake. The pH of each suspension was adjusted by the addition of sub-microliter quantities of 0.5 M NaOH and 0.5 M HCl to a range between 6.25 and 7.0, set at the midpoint between the pK_a of the microgels and the pK_a of each macromolecule. Experiments were run at pH 6.25 for dibucaine and pH 6.75 for benzylamine and doxorubicin.[20−22]

The resulting suspensions of microgels were then placed on an orbitron rotator II (model 260250, Boekel Industries, Inc.), until the system had reached equilibrium (in the sense that no change in absorbance of the supernatant was observed between 3, 5, and 7 h). Any shifts in pH after incubation were adjusted to the original pHs listed above by the addition of sub-microliter quantities 0.5 M NaOH and 0.5 M HCl. Finally, the suspensions were pelleted by centrifugation (RCF 3000) for 15 min (Marathon Micro A, Fisher Scientific).

Measurements of absorbance versus wavelength were made on the supernatant solutions of the drug/microgel suspensions and a control solution that contained drug but had never been exposed to the microgels. Appropriate dilutions were made to obtain absorbance readings in the linear range of Beer's law. The entire procedure was performed in triplicate for each drug and different composition microgel. The uptake of drug by the microgels (milliequivalents (mequiv) of drug per milligram of microgel) was calculated using eq 1

$$\text{uptake}\left(\frac{\text{mequiv of drug}}{\text{mg of microgel}}\right) = \frac{A_c - A_r}{A_c} C_{\text{stock}} \qquad (1)$$

where A_c and A_r are the absorbance of the control and reaction supernatant solution, respectively, and C_{stock} is the concentration at which the drug stock solution was prepared.

To measure the volume change of the microgels when they were loaded with the benzylamine, dibucaine, and doxorubicin, we used the micropipet flow technique described above. Individual microgels were immersed in test solutions that contained the drug, and their volume change was measured by video microscopy.

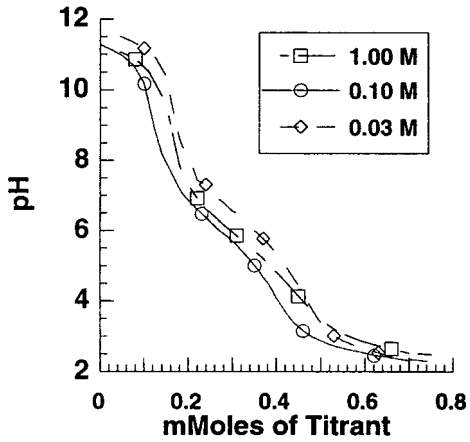

Figure 4. Plot of the bulk titration results for the carboxylic acid microgels run at NaCl concentrations of 0.020, 0.10, and 1.00 M.

Table 1. Summary of the Apparent pK_a's from the Bulk Titration of the Five Different Microgel Compositions

functional group	apparent pK_a	std deviation
carboxylic acid	4.67	0.25
glutamic acid	4.09	0.40
hydroxamic acid	6.57	0.42
ethanol	5.22	0.12
sulfonic acid	N/A	N/A

Experimental Results and Discussion

The experimental results and discussion is divided into four sections. In the first section we present the results of the bulk titrations, in the second section we present the pH swelling response, in the third section we present the NaCl swelling response, and in the fourth section we present the drug loading behavior.

Bulk Microgel Titrations. To determine the apparent pK_a and capacity of the different microgels, bulk titrations were performed. An expression for the apparent pK_a is given by eq 2:[7]

$$pK_{apparent} = pH_i + \log([Na^+]) - \log\left[\frac{X}{2}\right] \qquad (2)$$

where $[Na^+]$ is the bulk sodium concentration, $[X/2]$ is the concentration of ionizable groups when half of the polymer repeat units are protonated, and pH_i is the pH at the inflection point on the titration curve.

Figure 4 shows a sample plot of the bulk titration results for the carboxylic acid microgels at concentrations of 0.02, 0.1, and 1.00 M NaCl. From an analysis[5] of the bulk titrations of each microgel composition, averaged values for the inputs to eq 2 were obtained and used to calculate the microgels' apparent pK_a's (p$K_{apparent}$ in eq 2). As summarized in Table 1, this analysis yielded apparent pK_a's for microgels containing carboxylic acid (4.7), glutamic acid (4.1), hydroxamic acid (6.1), and ethanol (5.0) functional groups. When appropriate, the pK_a's of these functional groups in water at 25 °C are shown in Figure 1.[23] Taking into account the fact that all of the microgels had a baseline of ~40% carboxylic acid groups (based upon the feed ratio) that contributed to the measured apparent pK_a, there was excellent agreement between the microgels' measured pK_a's and the weighted average of the functional group pK_a's in solution. The apparent pK_a for the sulfonic acid microgels could not be measured by aqueous titration because of the strength of this acid group.

Table 2. Summary of the Capacities of the Five Different Microgel Compositions As Obtained from Bulk Titration Experiments

functional group	mquiv/g	std deviation
carboxylic acid	5.70	0.89
glutamic acid	7.90	0.43
hydroxamic acid	5.80	0.75
ethanol	3.61	0.25
sulfonic acid	N/A	N/A

Table 3. Density Results for Different Microgel Compositions Measured Using a 0.25 M Sucrose/Percoll Gradient

microgel composition	density (g/cm^3) ± 0.001 SD
carboxylic acid	1.0624
glutamic acid	1.0712
hydroxamic acid	1.0818
sulfonic acid	1.0625
ethanol	1.0618

Table 4. Loading Efficiencies (%) of Benzyl Amine, Dibucaine, and Doxorubicin into Each Microgel Composition[a]

microgel composition	benzylamine	dibucaine	doxorubicin
carboxylic acid	61	55	78
glutamic acid	68	54	72
hydroxamic acid	63	53	80
sulfonic acid	N/A	N/A	N/A
ethanol	96	67	105

[a] A loading efficiency could not be calculated for the sulfonic acid microgels because bulk titration data could not be obtained.

However, this fact was consistent with the pK_a of 1.8 for a sulfonic acid monomer in solution.[20]

The bulk titrations also provided information on the capacities ("capacity" = total number of functional ionic groups that bind protons) of the different composition microgels (Table 2). The capacity of the glutamic acid microgels increased by 37% from the carboxylic and hydroxamic acid microgels. This was a direct consequence of the fact that the replacement of carboxylic acid with glutamic acid groups in the post-polymerization reactions doubled the number of proton binding sites on the reacted polymer repeat units. In contrast, the capacity of the ethanol microgels decreased by 37% from the carboxylic and hydroxamic acid microgels. This was a direct consequence of the fact that the replacement of carboxylic acid with ethanol groups in the post-polymerization reactions eliminated the proton binding sites on the reacted polymer repeat units.

Swollen Microgel Densities. Table 4 lists the densities of the five different microgel compositions in their "swollen state" (implies that the gel contains polymer, solvent, and solute). These data show that the densities of all the gels are greater than that of water and within 1% of each other. The density of the swollen microgels containing carboxylic acid (pK_a = 4.7), sulfonic acid (pK_a = 1.8), and ethanol (pK_a = 5.2) were essentially the same (~1.062 g/cm^3) and were lower than the density of the swollen glutamic acid (pK_a = 4.09) microgels and hydroxamic (pK_a = 5.80) microgels. It was evident that the swollen density does not correlate with the pK_a's and hence the number of counterions. Since the different groups have different densities, and since the swollen gels may contain different amounts of water and ions, there is clearly a compensatory effect that involves the MW of derivatized units, the salt, and the amount of water present in the microgels.

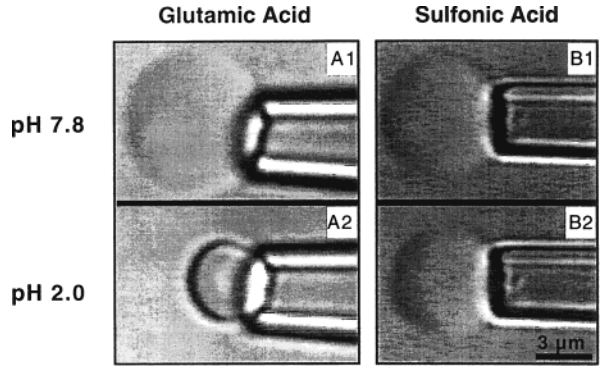

Figure 5. Video images of poly(methacrylic acid-*co*-acrylic acid) microgels held by micropipets and suspended in different pH citrate buffer solutions. (A1) Most expanded state: glutamic acid microgel in pH 7.8 buffer. (A2) Most condensed state: the glutamic acid microgel as A1 in a pH 2.0 buffer. (B1) Most expanded state: sulfonic acid microgel in pH 7.8 buffer. (B2) Most condensed state: the same sulfonic acid microgel as B1 in a pH 2.0 buffer.

To further characterize these microgels, we determined the density of the polymer in the microgels, ρ_p, in a manner independent of the solvent and solute contained in them. This was achieved by calculating ρ_p by noting that the density of the microgels in their swollen state, ρ_m, was equal to a weighted average (on a volume fraction basis) of the density of the aqueous solution in the microgels (ρ_s) and the polymer itself (ρ_p) (eq 3).

$$\phi_s\rho_s + \phi_p\rho_p = \rho_m \tag{3}$$

We used the measured swollen densities in Table 3 and a value of 1.032 g/cm^3 for ρ_s, the density of the 0.25 M sucrose solution at 25 °C.[23] The volume fractions of solvent (ϕ_s) and polymer (ϕ_p) in eq 3 were determined by taking the ratio of each of the microgels' dry volume to their maximum volume in 0.25 M sucrose as measured by video microscopy (see Methods). Substituting the measured densities for ρ_m in eq 3 and solving for ρ_p, we obtained the polymer density for each microgel.

The average polymer density in the carboxylic acid, hydroxamic acid, sulfonic acid, and ethanol microgels was 1.23 g/cm^3, a value slightly less than the density of the polymer in the glutamic acid microgels (1.29 g/cm^3). The densities measured by centrifugation (above) were approximately equal to the 1.22 g/cm^3 density of the dry polymer microgel that was measured using an alternate, but less accurate, method.[5] The previous method, which has large measurement errors associated with it, was based upon measurements of the microgels' dry mass and volume, from which we calculated their dry density.

Effect of Changes in Solution pH on Microgel Volume. Video images of two of the five different composition microgels (held by a micropipet) in pH 7.8 and pH 2.0 buffer are shown in Figure 5. From these images it is seen that both gel compositions are more expanded at pH 7.8 than at pH 2.0. Note that at the two pHs the size differential between the glutamic acid microgels is larger than that of the sulfonic acid microgels. This difference is due to the lower binding constant of protons to the sulfonic acid groups (pK_a = 1.8) as compared to the glutamic acid groups (pK_a = 4.4 and 3.1). The pH condensation of the microgels arises from the exchange of protons for sodium counterions that are

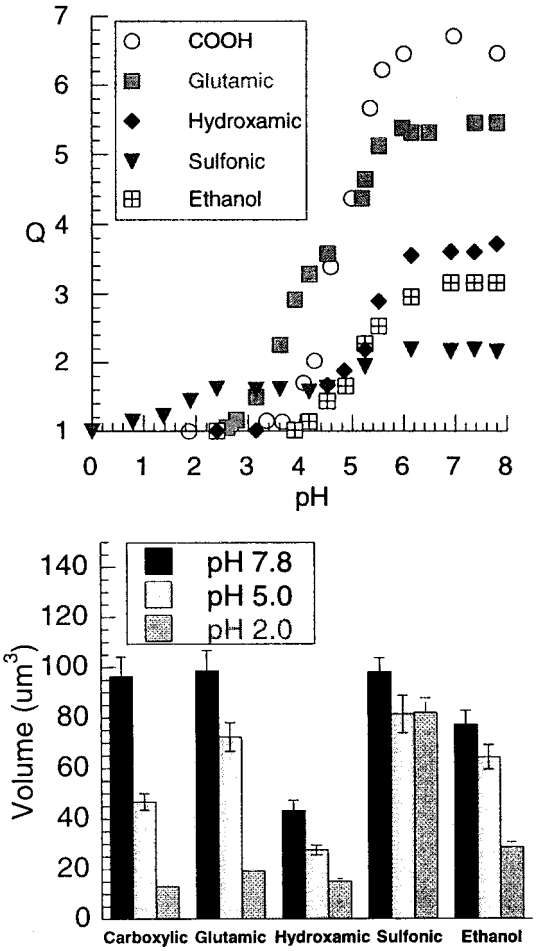

Figure 6. (a, top) Plot of the swelling ratio, *Q*, versus pH for all five microgel compositions as measured by the micropipet technique. (b, bottom) Plot of the diameters of all five microgel compositions in their fully swollen (pH = 7.8) and their most condensed (pH = 2.0) states.

associated with the fixed ionic groups in the microgel. The exchange and subsequent binding of protons to the fixed ionic groups results in a reduction in the osmotic swelling pressure inside the microgel and its subsequent reduction in volume (discussed in more detail below).[7] Thus, at pH 2.0, the sulfonic acid microgels remained swollen because, in contrast to the carboxylic acid groups that were bound with protons, their functional groups remained ionized.

Figure 6a contains a plot of the equilibrium swelling ratio *Q* (the ratio of the volume of a microgel at the test pH to its minimum volume) versus the bulk pH for all five microgel compositions. It is important to recognize that the results in Figure 6a represent relative changes in volume due to the pH response and so do not reflect absolute volume changes for the different sized microgel compositions. To compare the actual magnitude of the swelling responses for each composition, it was necessary to plot the average volume of the microgels at low and high pH (Figure 6b). In the sections that follow, we analyze the ranges of the swelling responses for each microgel composition using the results in Figure 6a and the magnitude of the swelling response using the results in Figure 6b. Note that, on the basis of the monomer feed ratio, it follows that 40% carboxylic acid functional groups were present in all of the microgel compositions.

Carboxylic Acid Microgels. For the carboxylic acid microgels, Figure 6a shows that for pH's < 3.6 the

microgels reached their minimum aqueous volume and for pH's > 5.3 they were in their most expanded state (7 times the minimum volume). The swelling transition for the carboxylic acid microgels was centered on a pH of 4.6, a value consistent that obtained from the titration experiments where $pK_a = 4.7 \pm 0.25$ (SD) (Table 2).[5] The results in Figure 6b show that increasing the pH from 2.0 to 7.8, while holding the buffer ion concentration constant, caused the microgel volume to increase 83.4 μm^3 from 13.0 ± 0.6 to 96.4 ± 7.8 μm^3 (±SD).

Glutamic Acid Microgels. For the glutamic acid microgels, the results in Figure 6a show that at pH's < 2.9 the microgels reached their minimum volume and at pH's > 5.3 they were in their most expanded state (5 times the minimum volume). Two distinct volume transitions were observed because of the presence of both carboxylic acid and glutamic acid functional groups on the microgels. The first transition was centered at pH 4.6 and the second one at pH 3.7. The average of these two transitions was 4.1, which was in good agreement with the apparent pK_a of 4.1 ± 0.4 (SD) measured using bulk titration (Table 1). Thus, the net effect of derivatizing the microgels with glutamic acid was to lower the overall swelling transition by 0.6 pH units.

The results in Figure 6b show that increasing the pH from 2.0 to 7.8, while holding the buffer ion concentration constant, caused the average glutamic acid microgel volume to increase 79.5 μm^3 from 19.1 ± 1.7 to 98.5 ± 8.1 μm^3 (±SD). We found that the glutamic and carboxylic acid microgels have a comparable volume at pH 7.8 but that the glutamic acid microgels were 1.5 times larger at pH 2.0. The fact that the volumes of the glutamic and carboxylic acid microgels were comparable at pH 7.8, despite an increased osmotic pressure in the glutamic acid microgels, suggests that both microgel compositions had reached their elastic limit. One explanation for the larger volume of the glutamic acid microgels at pH 2.0 was that the glutamic acid functional groups occupied a larger volume than the carboxylic acid functional groups and thereby sterically limited the collapse of the microgels.

Ethanol Microgels. For the ethanol microgels, the results in Figure 6a show that at pH's < 4.2 the microgels reached their minimum aqueous volume and at pH's > 6.0 the microgels were in their most expanded state (2−3 times the minimum volume). Since ethanol does not carry a charge and thus does not contribute to the expanding pressure, it was the presence of carboxylic acid groups that induced the volume transition. The ethanol microgel volume transition was centered on a pH of 5.1, which was consistent with their apparent pK_a of 5.0 ± 0.2 that was measured by bulk titration (Table 1). When compared with the carboxylic acid microgels, the net effect of derivatizing the microgels with ethanol was to increase the swelling transition by 0.4 pH units. An explanation for the 0.4 unit increase in the pH of the volume transition was that the ethanol functional groups lowered the dielectric constant in the microgels and thereby increased the pH gradient that was required to swell the microgels.

The results in Figure 6b show that increasing the pH from 2.0 to 7.8, while holding the buffer ion concentration constant, caused the average ethanol microgel volume to increase 48.4 μm^3 from 28.7 ± 5.5 to 77.1 ± 2.1 μm^3 (±SD). We observed that the ethanol microgels' volume was 2.2 times larger than the volume of the carboxylic acid microgels at pH 2.0 and 0.8 times smaller than their volume at pH 7.8. We hypothesize that the ethanol microgels' increased volume at pH 2.0 compared to that of the carboxylic acid microgels was due to the fact that water was a better solvent for ethanol functional groups than the smaller protonated carboxyl groups. The smaller volume of the ethanol microgels at pH 7.8 compared to that of the carboxylic acid microgels can be explained by the fact that there were fewer ionic functional groups and as a result less of an osmotic swelling pressure in these microgels. Thus, in view of one of our original goals, to reduce the magnitude of the swelling response, we were successful in the case of the ethanol microgels.

Hydroxamic Acid Microgels. For the hydroxamic acid microgels, the results in Figure 6a show that at pH's < 4.2 the microgels reached their minimum aqueous volume and at pH's > 6.0 were in their most expanded state (~3.5 times the minimum volume). These microgels exhibited two very distinct volume transitions that arise as a consequence of the distinct pK_a's of the carboxylic acid and hydroxamic acid functional groups. The first volume transition was centered on a pH of 5.8 (hydroxamic acid) and the second on a pH of 4.7 (carboxylic acid). The average of these two volume transitions was 5.25, which was consistent with the apparent pK_a of 5.7 ± 0.5 measured by bulk titration. When compared with the carboxylic acid microgels, the net effect of derivatizing the microgels with hydroxamic acid was to increase the swelling transition by 0.5 pH units.

The data in Figure 6b show that increasing the pH from 2.0 to 7.8, while holding the buffer ion concentration constant, caused the average hydroxamic acid microgel volume to increase 28.3 μm^3 from 15.0 ± 2.2 to 43.3 ± 4.2 μm^3 (±SD). We observed that the hydroxamic and carboxylic acid microgels had comparable volumes at pH 2.0 but that the hydroxamic acid microgels were 0.45 times smaller at pH 7.8. In addition, the polymer volume fraction in the hydroxamic acid microgels (as determined by comparing the microgels' dry volume to their swollen volume using video microscopy) was higher ($\phi = 0.25$) than that of three of the other compositions tested ($\phi < 0.13$). We hypothesize that the higher polymer concentration of the hydroxamic acid microgels increased the probability of the formation of short-range interactions. Strong hydrogen bond formation between the nitrogen and hydrogen on the hydroxamic acid groups and the oxygens on the carboxylic acid functional groups could have limited the extent to which the microgels could take up water and swell at higher pH.

Sulfonic Acid Microgels. For the sulfonic acid microgels, the results in Figure 6a show that in solutions with pH's > 6.0 the microgels were in their most expanded state (~2 times the minimum volume). However, the microgels remained partially swollen even at pH's < 1.0. Even though their volume transitions were small, because of the presence of both carboxylic acid and sulfonic acid functional groups on these microgels, there were two distinct volume transitions between pH 0.0 and pH 7.8. The first volume transition was centered on a pH of 5.1 (carboxylic acid) and the second on a pH of 1.8 (sulfonic acid).

The results in Figure 6b show that increasing the pH from 2.0 to 7.8, while holding the buffer ion concentration constant, caused the average sulfonic acid microgel volume to increase16 μm^3 from 81.7 ± 5.9 to 98.0 ± 5.7

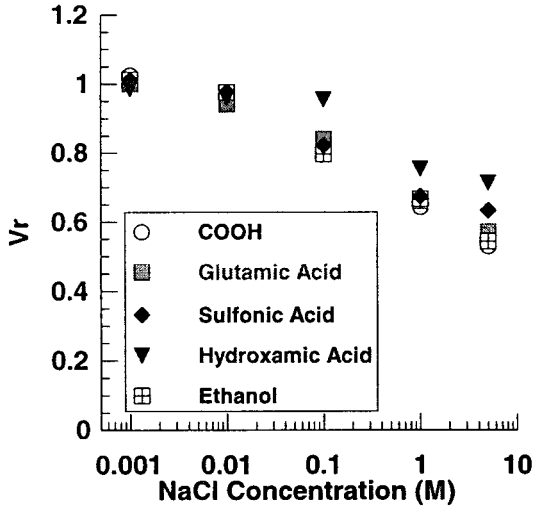

Figure 7. Plot of Vr in the presence of 0.01, 0.1, 1.0, and 5 M NaCl for all five microgel compositions.

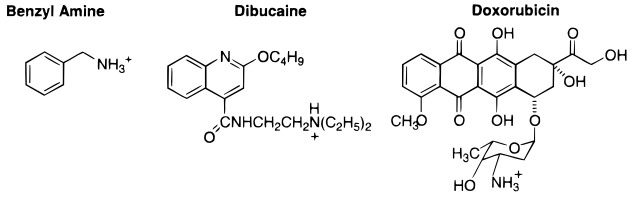

Figure 8. Molecular structures of the drugs used in the loading studies.

μm^3 (±SD). We observed that the sulfonic and carboxylic acid microgels had comparable volumes at pH 7.8 but that the sulfonic acid microgels were 6.3 times larger at pH 2.0. We hypothesize that this was a result of the fact that the sulfonic acid groups remained ionized at this pH and thus exerted an osmotic pressure that caused the gels to remain swollen.

Effect of Changes in NaCl Concentration on Microgel Volume. Figure 7 shows a plot of Vr, the ratio of the microgel's volume at pH's > 5.3, to their maximally swollen volume (in 1 mM NaCl), plotted against the NaCl concentration. With the exception of the hydroxamic acid microgels at NaCl concentrations ≥0.1 M, no significant differences were observed between the Vr's for the other three hydrogels as a function of NaCl concentration. The higher Vr's for the hydroxamic acid microgels can be explained by the fact that the hydroxamic acid microgels were markedly collapsed under the test conditions (pH 7.8; see Figure 6b). Changing the suspending solution's ion concentration to 5 M NaCl produced the largest salt induced change in volume. The maximum reduction in volume in the presence of sodium chloride was much less than the Vr that was measured when we lowered the pH (Vr = 0.15, 0.19, 0.27, 0.45, and 0.30 for the carboxylic acid, glutamic acid, hydroxamic acid, sulfonic acid, and ethanol microgels). A primary reason for this difference was that the functional groups' binding constants for protons (as determined by their pK_a's) were greater than their binding constants for sodium ($K_d \sim 0.1$ M[5]). Therefore, in the presence of sodium and its associated waters of hydration the ionized functional groups generated a larger osmotic swelling pressure.[5,24]

Drug Loading. Figure 8 shows the molecular structures of the three cationic drugs[21,22,25] that were loaded into the microgels. These compounds were chosen because of their potential therapeutic value, similarity in being monovalent cationic weak bases, and increasing size, water solubility, and chemical complexity.

Table 5. Molecular Volumes and the Octanol−Water Partition Coefficients (log *P*) of Benzyl Amine, Dibucaine, and Doxorubicin[26] [a]

drug/molecule	vol (cm^3)	octanol/water partition coeff (log *P*)	amount loaded (mequiv/g)
proton	N/A	N/A	5.70
benzylamine	27.6	1.07	4.13
dibucaine	135.5	1.85	3.22
doxorubicin	450.5	2.52	4.86

[a] Also listed are the results of the average amount of the molecules that loaded into the microgels.

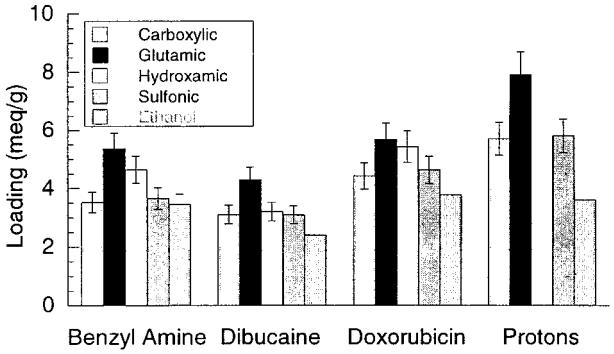

Figure 9. Plot of the drug loading into the five different composition microgels.

Table 4 lists the percent loading efficiencies (percent loading efficiency is defined as the ratio of drug loaded to protons loaded × 100) of the drugs into the microgels. All of the loading efficiencies in Table 4 were less than or equal to 100%. This indicated that the maximum loading capacity for all of the microgels depended on the capacity of the microgels (measured by bulk titration) as well as a variety of other factors including the H-bonding ability and partitioning coefficients of the drugs (see below).

From the results in Table 5, it was evident that the loading of the three molecules was not dependent on their volumes. The average loading levels (into all five compositions) for doxorubicin, benzylamine, and dibucaine were 4.86, 4.13, and 3.22 mequiv/g, respectively (significantly different, *t*-test, alpha = 0.05). Thus, doxorubicin, the molecule with the largest volume = 450 Å^3, had the highest average loading across compositions, benzylamine, the molecule with the smallest volume = 27.6 Å^3, had the second highest level of loading and dibucaine, volume = 135.5 Å^3, had the lowest average loading. The independence of the average loading on the volume of the molecules suggested that steric effects alone could not explain the different degrees of loading. Other factors that could have played a role were differences in the relative binding affinity of the molecules for the ionic groups in the gels or the degree of intermolecular bonding interactions between molecules (discussed in more detail below).

We will now examine and compare the degree of drug loading for each of the five microgel compositions (Figure 9).

Carboxylic Acid Microgels. The loading of benzylamine, dibucaine, and doxorubicin into the microgels with 100% carboxyl groups was 3.52, 3.11, and 4.42 mequiv/g, respectively (protons = 5.7 mequiv/g). The

carboxylic acid microgels will serve as the baseline to which the degree of loading of all of the other compositions will be compared.

Glutamic Acid Microgels. The loading of benzylamine, dibucaine, and doxorubicin into the glutamic acid microgels was 52%, 38%, and 28% higher, respectively, than their loading into the carboxylic acid microgels. This result was consistent with the 40% higher capacity of the glutamic acid gels that was measured by bulk titration (protons = 7.9 mequiv/g).

Hydroxamic Acid. The average loading of all three molecules into the hydroxamic acid microgels was statistically equivalent (*t*-test, alpha = 0.05) to that of the carboxylic acid microgels. This result was consistent with the comparable 5.8 and 5.7 mequiv/g proton capacities of the hydroxamic acid and carboxylic acid microgels, respectively, that were measured by bulk titration.

Sulfonic Acid. For the sulfonic acid microgels the loading of benzylamine, dibucaine, and doxorubicin was 31%, 3%, and 22% higher, respectively, than the carboxylic microgels. We speculate that the higher levels of loading in the cases of the benzylamine and doxorubicin were due to the fact that the sulfonic groups bind these molecules more strongly than the carboxylic groups.

Ethanol. The loading of benzylamine, dibucaine, and doxorubicin into the ethanol microgels decreased by 2%, 23%, and 7%, respectively, from that of the carboxylic acid microgels. This decrease was consistent in direction though not in magnitude with the 40% reduction in proton uptake (measured by bulk titration) between the ethanol and carboxylic acid microgels.

To try to explain this inconsistency, we compared the loading efficiencies (loading efficiency was defined as the ratio of drug loaded to protons loaded) of each of the drugs into the ethanol microgels with their loading efficiency into the other four microgel compositions (Table 4). We found that in all cases the ethanol microgels had a higher loading efficiency than the other microgel compositions. For benzylamine the loading efficiency into the ethanol microgels was 96% versus 68% for the next highest microgel composition. For dibucaine the loading efficiency was 67% versus 55% for the next highest microgel composition. For doxorubicin the loading efficiency was 100% versus 80% for the next highest microgel composition. We hypothesize that the ethanol microgels had a higher loading efficiency because their ionic functional groups were more widely distributed in the polymer network. As a result, more of the ionic sites remained accessible (i.e., the drugs were not sterically restricted from approaching neighboring binding sites) when the drugs bound to and collapsed the network.

Volume Response. To further understand the source of the differences in loading behavior, we used the micropipet flow technique to measure the volume changes of the five different microgel compositions when they were loaded with each of the cationic molecules (Figure 10). We observed that there were no significant differences in Vr as a function of microgel composition for the loading of any of the drugs. The fact that there were different degrees of loading across microgel compositions, but identical changes in volume for a given drug, indicated that volume constraints were not a determining factor in setting the degree of loading across compositions.

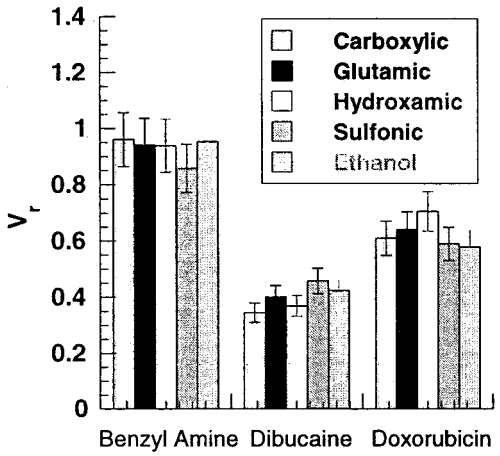

Figure 10. Plot of Vr for the five microgel compositions loaded with benzylamine, dibucaine, and doxorubicin.

Although the volume changes of all five compositions were the same for a given drug, they were different between drugs. The different volume condensing effects of these drugs have been discussed in detail in previous work and thus will only be discussed briefly here.[13] When loaded with benzylamine, doxorubicin, and dibucaine the average Vr's for all five compositions were different (0.9, 0.6, and 0.4, respectively). To explain the differences in the magnitude of these volume changes, we examined the octanol−water partition coefficients, log *P* (Table 5),[26] of benzylamine, doxorubicin, and dibucaine, which were 1.07, 1.85, and 2.52, respectively. These partition coefficients indicated that it was more thermodynamically favorable for dibucaine to reside in a less polar environment than benzylamine. Thus, dibucaine, which had the highest partition coefficient, dehydrated the microgels the most (Vr = 0.4), and benzylamine, which had the smallest partition coefficient, condensed the microgels the least (Vr = 0.6).

Model Results and Discussion

Model To Predict the Equilibrium pH Swelling Response. One goal of this work was to obtain a quantitative explanation for the swelling versus pH curves shown in Figure 6. To achieve this goal, we have modified an existing thermodynamic model for the swelling of ionic polymer networks[2,27] to predict the pH swelling response of the microgels as a function of their functional group composition. The modified model has been described in detail previously,[13] and we will only give a brief description here. The modified model contained three important modifications: (1) it included a term to account for counterion binding to the matrix, which was necessary to account for the high density of fixed charges in the microgels (~2.5 M); (2) it included a term to account for the change in solubility of the microgels with pH/polymer volume fraction and entailed using a variable Flory χ parameter; and (3) it used a non-Gaussian expression for the elasticity to account for the high cross-linking density in the microgels (9.5 monomers between cross-links based upon the previously measured pore size).[13]

Model Inputs. The inputs that were used in the model are summarized in Table 6. For each of the microgel compositions, ρ, the density of pure polymer in the microgels, was obtained from their experimental density measurements (Table 3). The polymer repeat unit average molecular weight was estimated using a

Table 6. Values That Were Used as the Model Inputs

variable	value	source
K_a(COOH)	$10^{-4.7}$	measured
K_a(glutamic)	$10^{-4.1}$	measured
K_a(ethanol)	$10^{-5.0}$	measured
K_{Na}	0.25	Smith, R.; et al. (1997)
C_{Na}	0.03 M	experimentally set
ρ(polymer)	0.97 cm^3/g	Handbook
polymer repeat unit avg MW	86 g/mol	calculated based upon feed ratio of monomer
ϕ_0	0.8	measured
V1	18 cm^3/mol	CRC
χ(carboxyl and glutamic)	$0.45 + 0.489\phi$	literature[33]
χ(ethanol)	$0.25 + 0.489\phi$	
$C_{carboxyl}$	5.77 mequiv/g	measured
$C_{glutamic}$	3.60 mequiv/g	measured
$C_{ethanol}$	7.20 mequiv/g	measured
$N-0.20$ feed ratio	9.5	measured[13]

weighted average molecular weight of the monomers used in the synthesis. This calculation took into account the number of repeat units between cross-links, N, and included the molecular weight of a single MBAM cross-linking monomer. The value for ϕ_0 (=0.80), the ratio of the microgels' dry volume to their condensed volume, was measured by video microscopy and was the same within experimental measurement error (±0.02) for all of the different cross-linking density microgels. The functional relationship that was used for χ is given by eq 4:

$$\chi = \chi_0 + b\phi \tag{4}$$

where χ_0 is the Flory parameter of the polymer at infinite dilution and b is the slope.[13] Because no experimentally measured values exist for the concentration dependence of the Flory parameter of our microgels, we made a reasonable estimate based upon the results for several comparable polymer systems.[28−32] Following previous work we used values of 0.45 and 0.489 for χ_0 and b, respectively, in the carboxylic and glutamic acid microgels. Values of 0.25 and 0.489 were used in the case of the ethanol microgels based on a weighted average for χ_0 and b of poly(vinyl alcohol) polymers and those of methacrylic acid polymers. The number of functional groups in a known mass of microgels was measured by bulk titration for each of the different composition microgels. The apparent pK_a's of the microgels were also measured by bulk titration. The polymer volume fractions that were predicted by the model at each pH were referenced to the polymer volume fraction of the microgels in their most condensed state. Finally, the values for N, the number of monomers between cross-links, were deduced from experimental measurements on gels' pore sizes in previous work[13] and were the same for the different composition gels since they all came from the same initial polymerization reaction.

Model Predictions of the pH Swelling Response and Comparison with Experiment. The model predictions and experimental results of the pH swelling curves for the ethanol, carboxylic acid, and glutamic acid microgels are presented in Figure 11. The data show that there was good quantitative agreement between theory and experiment ($R^2 \geq 0.95$) over the entire pH range. The model did not capture the multiple pK_a's of the glutamic acid microgels response (although it could be modifed to do so). However, it captured the most important features of the swelling response, i.e., the shift in the range and magnitude of the swelling response. The agreement between the model and experiment indicated that the model has predictive, correlative, and design capabilities.

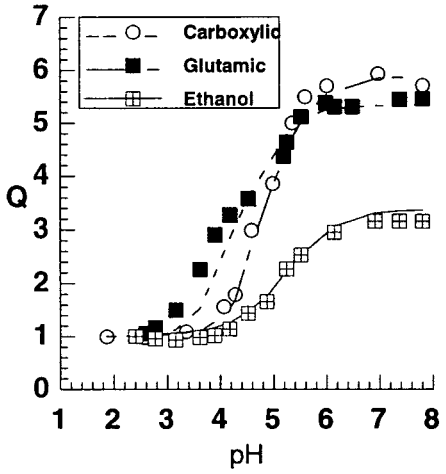

Figure 11. Plot of the model predictions for the microgels' pH swelling response and comparison with experiment.

Conclusion

The experimental work presented here provides quantitative data regarding how changing the functional groups on gels will alter their responses to pH, NaCl, and their ability to load particular drugs. We found that the pH range was shifted by an amount proportional to the solution pK_a's of the functional groups that were derivatized to the polymer backbone. Although the capacity of the microgels as measured by proton uptake and drug loading increased in proportion to the number of additional functional groups per polymer repeat unit, it did not decrease when the number of functional groups was lowered. This was a consequence of improved loading efficiency for the ethanol derivatized microgels. The selectivity of the gels for the specific drugs studied was independent of the functional group composition for the drug/functional group pairs studied. This indicated that additional research is needed to elucidate how microgels can be engineered to be selective for a given drug. Finally, we used Flory−Huggins theory, modified to account for ion binding, the change in the Flory interaction parameter with swelling, and the non-Gaussian elasticity of the microgel matrix, to quantitatively predict the equilibrium swelling of the microgels as a function of pH. The agreement between the model and experiment suggested that the model has correlative, design, and predictive capabilities.

Acknowledgment. The authors thank Professors Andrey Dobrinyin, George Pearsall, Michael Rubinstein, and Doncho Zhelev for helpful discussions. The authors gratefully acknowledge financial support from the Duke University Center for Cell and Biosurface Engineering NIH Training Fellowship, North Carolina Space Grant Consortium, Access Pharmaceuticals, NIH-GM 27278 and NIH-GM 40162.

Appendix: Nomenclature

A	number of monomers between uncondensed charges
A_c	absorbance of the control solution
A_r	absorbance of the supernatant in the reaction solutions

b	the slope for the functional dependence of the χ parameter on ϕ
c	monomer concentration (number density)
c_s	salt concentration (number density of each monovalent salt ion)
k	Boltzmann's constant
M_c	polymer repeat unit average molecular weight
N	number of monomers in a gel strand
P	octanol−water partition coefficient
Q	equilibrium swelling (ratio of a fully swollen gel volume to its condensed volume)
Q_{max}	maximum equilibrium swelling ratio in pH 7.8 buffer, 0.01 M NaCl
T	temperature
V_r	ratio of the microgel volume in the presence of a given pH, NaCl, and or drug concentration fully swollen microgel volume in pH 7.8 buffer, 0.001 M NaCl
χ	Flory interaction parameter
χ_0	Flory interaction parameter at infinite dilution
ϕ	volume fraction of polymer
ρ	density of polymer

References and Notes

(1) Tanaka, T.; Fillmore, D.; Sun, S.; Nishio, I.; Swislow, G.; Shah, A. *Phys. Rev. Lett.* **1980**, *45*, 1636−1639.
(2) Shibayama, M.; Tanaka, T. *Adv. Polym. Sci.* **1993**, *109*, 1−62.
(3) English, A.; Mafe, S.; Manzanares, J.; Yu, X.; Grosberg, A.; Tanaka, T. *J. Chem. Phys.* **1996**, *104*, 8713−8720.
(4) Miyata, T.; Nakamae, K.; Hoffman, A.; Kanzaki, Y. *Macromol. Chem. Phys.* **1994**, *195*, 1111−1120.
(5) Eichenbaum, G.; Kiser, P.; Simon, S.; Needham, D. *Macromolecules* **1998**, *31*, 5084−5093.
(6) Kiser, P.; Wilson, G.; Needham, D. *Nature* **1998**, *394*, 459−462.
(7) Helfferich, F. *Ion Exchange*; McGraw-Hill Book Company: New York, 1962.
(8) Kim, S.; Bae, Y.; Okano, T. *Pharm. Res.* **1992**, *9*, 283−290.
(9) Langer, R. *Ann. Biomed. Eng.* **1995**, *23*, 101−111.
(10) Peppas, N. *Hydrogels in Medicine and Pharmacy;* CRC Press: Boca Raton, FL, 1986; Vol. I.
(11) Hasa, J. *J. Polym. Sci., Polym. Phys. Ed.* **1975**, *13*, 253−262.
(12) Hoffman, A. S. In *NATO ASI Series*; Piskin, E. a. H. A. S., Eds.; Martinus Nijhoff Publishers: Dordrecht, 1986; Vol. 106.
(13) Eichenbaum, G.; Kiser, P.; Dobrynin, A.; Simon, S.; Needham, D. *Macromolecules* **1999**, *32*, 4867−4878.
(14) Kawaguchi, H.; Kawahara, M.; Yaguchi, N.; Hoshino, F.; Ohtsuka, Y. *Polym. J.* **1988**, *20*, 903−9.
(15) Kashiwabara, M.; Fujimoto, K.; Kawaguchi, H. *Colloid Polym. Sci.* **1995**, *273*, 339−345.
(16) Morawetz, H.; Zimmering, P. *J. Phys. Chem.* **1954**, *53*, 753.
(17) Gaetjens, E.; Morawetz, H. *J. Am. Chem. Soc.* **1960**, *82*, 5328.
(18) Kepley, C.; Craig, S.; Schwartz, L. *J. Immunol. Methods* **1994**, *175*, 1−9.
(19) Braet, F.; DeZanger, R.; Sasaoki, T. *Lab. Invest.* **1994**, *70*, 944−952.
(20) Loudon, G. *Organic Chemistry*, 2nd ed.; Benjamin/Cummings Publishing Company Inc.: Menlo Park, CA, 1988.
(21) Padmanabhan In *Analytical Profiles of Drug Substances*; Florey, K., Ed.; Academic Press: New York, 1983; Vol. 12, pp 105−134.
(22) Arcamone, F. *Doxorubicin: Anticancer Antibiotics*; Academic Press: New York, 1981.
(23) *CRC Handbook of Chemistry and Physics*, 71st ed.; Lide, D., Ed.; CRC Press: Boston, 1990.
(24) Gregor, H. *J. Am. Chem. Soc.* **1951**, *73*, 643−650.
(25) *Burger's Medicinal Chemistry*, 4th ed.; Wolff, M., Ed.; John Wiley & Sons: New York, 1981; Vol. 3.
(26) Meylan, W.; Howard, P. *J. Pharm. Sci.* **1995**, *84*, 83−92.
(27) Brannon-Peppas, B. L. a. P.; Nikolaos, A. *Chem. Eng. Sci.* **1991**, *46*, 715−722.
(28) Mikos, A.; Peppas, N. *Biomaterials* **1987**, *9*, 419−423.
(29) Kopecek, J.; Bazilova, H. *Eur. Polym. J.* **1974**, *10*, 465−470.
(30) Hasa, J. *J. Polym. Sci., Polym. Phys. Ed.* **1975**, *13*, 263−274.
(31) McKenna, G.; Korkay, F. *Polymer* **1994**, *35*, 5737−5742.
(32) McKenna, G.; Flynn, K.; Chen, Y. *Polym. Commun.* **1988**, *29*, 272−275.
(33) Bohdanecky, M.; Bazilova, H.; Kopecek, J. *Eur. Polym. J.* **1974**, *10*, 405−410.

MA9908393